Vol. 05, No. S1 (2023) 27-34, doi: 10.24874/PES.SI.01.004

Proceedings on Engineering Sciences

www.pesjournal.net

EFFICIENT POWER HARVESTING FOR FUEL CELLS: DYNAMIC-STEPPED MPPT WITH NEURAL ADAPTIVE WATER CYCLE METHOD

Shubhendra Pratap Singh[1]
Beemkumar N.
Ganesh Kumar Kantak

Received 15.04.2023.
Accepted 20.06.2023.

Keywords:

Fuel cell, power harvesting, MPPT, neural adaptive water cycle (NA-WC), optimum power output.

A B S T R A C T

In this research, a new approach based on a dynamic-stepped maximum power point tracking (MPPT) technology and a neural adaptive water cycle (NA-WC) method is proposed to improve the power gathering effectiveness of fuel cells. Although fuel cells have drawn a lot of interest as a clean and effective energy source, maximizing their power harvesting effectiveness is still a major problem. To solve this problem, we present a brand-new dynamic-stepped MPPT method that constantly alters the fuel cell's functioning position to achieve optimum output of power under various environmental circumstances. A 7 kW proton-exchange membrane fuel cell (PEM-FC) that supplied a resistive load through a boost converter created utilizing the suggested MPPT controller was effectively used to study the effectiveness of the suggested NA-WC MPPT. The suggested NA-WC outperforms the traditional MPPT approaches in terms of convergence rate, overshoot, and steady state fluctuations, according to simulation findings obtained by utilizing the Matlab tool. Additionally, the fuel cell's lifespan and effectiveness can both be increased by the suggested controller's current ripple minimization.

1. INTRODUCTION

Electrochemical devices known as fuel cells provide an ecological and effective way to transform chemical energies into electricity. Due to their high energy conversion efficiency, minimal emission levels, and adaptability in a wide range of uses, they have generated substantial interest as a possible substitute for traditional sources of energy. However, it is essential to concentrate on raising the effectiveness of their power collecting if fuel cells are to reach their full capacity (Gul et al., (2021)). Fuel cells work on the basis of electrochemical processes, in which an oxidizing agent, usually oxygen from the air, combines with a fuel source, such as hydrogen, to create heat, water, and electricity. The fuel cell system, which consists of several separate cells linked in either parallel or series, is where this procedure occurs. The electrodes, catalysts, and an electrolyte are some of the parts that make up the chain and help to speed up processes and transport of ions (Liang et al., (2017)). Efficiency is a crucial component of fuel cell technology since it

[1] Corresponding author: Shubhendra Pratap Singh
Email: shub.pratap16@gmail.com

impacts the system's general efficiency and financial sustainability. The fuel cell's capacity to efficiently transform chemical energy from the fuel into electrical energy is referred to as energy harvesting effectiveness. An increase in effectiveness results in increased power production for a given quantity of fuel ingested, which improves the environment and lowers costs. A number of things affect a fuel cell's performance (Chong et al., (2019)).

The catalyst substance employed in electrodes is one important factor that improves the kinetics of electrochemical processes by offering areas of activity for those reactions. Due to their significant action, platinum-based catalysts like platinum black or platinum nanoparticles are frequently a fuel cell technology used in PEM-FCs. Yet, because of prices and insufficient availability, non-precious metallic catalysts have been developed as a substitute catalytic substance to increase effectiveness and lower costs. The effectiveness of the electrolyte or membrane is another significant factor that significantly affects fuel cell performance (Jadhav et al., (2021)). While avoiding the mingling of fuel and oxidizer gases, the membrane permits the transfer of ions between the electrodes. Improvements in membrane materials, such as the creation of hybrid films or proton-conductive polymers, have boosted ion conductivity, and decreased opposition, and increased performance as a whole. The best system configuration and performance are also necessary for effective electricity collecting. This entails the right sizing and arrangement of the fuel cell stack, as well as the balance-of-plant elements and auxiliary systems like refrigeration and humidity (Bizon et al., (2017)).

This paper proposes a NA-WC MPPT controller for fuel cell power systems. It was feasible to test the efficacy of the neural network MPPT utilizing a 7 kW PEM-FC that delivered reactive loads utilizing a booster conversion developed with the recommended MPPT regulator.

The remainder of the paper is divided into subsequent parts. In part 3 the PEMFC and Proposed method are explained. The part 4 contains the simulation results and related discussions, while the Part 5 discusses the main conclusions drawn from our study.

2. LITERATURE REVIEW

The utilization of nano-particles to harness renewable energy sources along with associated technology like the manufacture of hydrogen, solar cells, geothermal power, and biofuel are the main topics of this study (Ahmadi et al., (2019)). Tang et al., (2019) examined the effects of cathode temperatures and microbial fuel cell (MFC) connection kinds on the efficiency of sewage treatment and generation of electricity in a 30 L pilot-scale built wetlands-microbial fuel cell (CW-MFC). Rezk et al., (2021) suggested an enhanced "fuzzy logic control (FLC)" system design methodology for MPPT control of PEM-FCs. The recommended architecture is based on the just published Balance Analyzer technique for determining the ideal settings that maximize the built-in versatility and liberty of FLC structures in addition to enabling rapid and accurate monitoring. In order to improve the optimum power recovery of FCs, this work provides an improved fuzzy-logic MPPT approach that utilizes the differential evolution optimization algorithm (DEOA) (Aly and Rezk, (2020)). Aly and Rezk, (2022) presented a FLC MPPT technique for improving the functioning of PEM-FC systems. Electricity, quantity of water, and warmth are the three detectors used in the literature's standard MPPT approaches. Artificial Neuro-Fuzzy Inference System (ANFIS), altered Hill-Climb with Fuzzy Logic Controller (MHC-FLC), Perturb and Maintain with "Practical Swarm Optimization (P&O-PSO)", and "Adaptive Cuckoo Search (ACS)" are the five different soft- Computing MPPT techniques that were examined (Hussaian Basha and Rani, (2020)). Haq et al., (2022) described a nonlinear generalization global sliding mode controller (GGSMC) that uses a DC-DC buck-boost converter to extract the most power possible from a PV array. As an initial electricity, a feed-forward neural network (FFNN) is employed. (Sarhan et al., (2017) MPPT approaches utilizing ANN and "adaptive neuro-fuzzy systems (ANFIS)" are used to regulate a grid-connected PV system. Regarding their performance effectiveness and sensitivity to changes in solar radiation and cell temperatures, both suggested MPPT techniques are examined. For fuel cell-based electric vehicle programs, this study paper presents a "chicken swarm optimization (CSO)"-based MPPT. By using a bi-directed conversion with natural clamp zero current changing, the need for active snubber elements is removed, which lowers the loss of switching (Priyadarshi et al., (2021)). Luta and Raji, (2019) examined two Maximum Power Point Tracking (MPPT) methods, one founded on the Particle Swarm Optimisation (PSO) algorithm and the other on the Mamdani Fuzzy Inference System, to keep a fuel cell stack's output power very near to its optimum.

3. METHODOLOGY

3.1 Illustration of PEM Fuel Cell

The major part of a fuel cell's technology is an electrolyte membrane, which is made up of two electrodes (known as the anode and cathode). Pressurized O_2 and H_2 are used to provide it in order to create energy. The hydrogen splits into protons and electrons in the anode. Since only protons can enter across the electrolyte membrane, electrons must go via an outside force to generate energy before arriving at the cathode side, where they are going to join the protons. H_2 Separations interact with O_2in the cathode to create heat and water (vapor). Figure 2 depicts a

single cell's efficiency under typical pressure and temperature conditions. Additionally, this graph shows the variances between the actual operating voltage and the ideal voltage value. It is seen that the voltage initially drops, then acts linearly, and then experiences a precipitous fall at a greater current intensity. The three primary polarizing losses—activation, ohmic, and concentration—are to blame for this voltage differential.

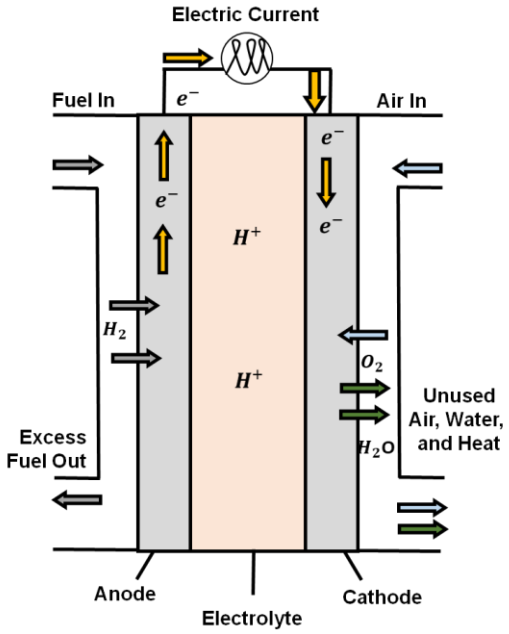

Figure 1. Illustration of PEM Fuel Cell

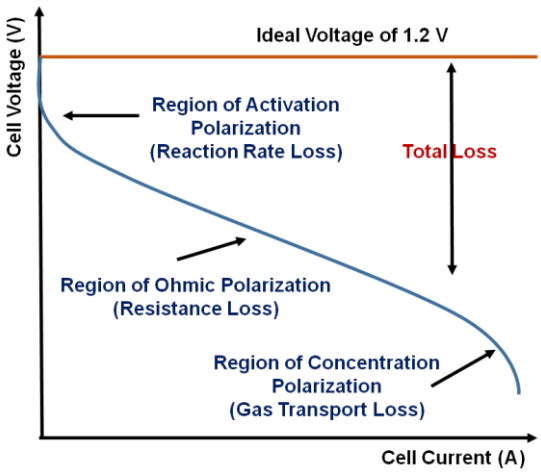

Figure 2. Differences between the ideal and actual fuel cell voltage

A strong non-linear behavior defines an activating polarization loss. This is a result of the PEMFC electrode's response dynamics. Because of the lengthy duration and ongoing operation of the chemical process, the activation polarization is significant at low voltage densities (primarily affecting in the beginning section of the polarization curve). The ohmic energy losses caused by the membrane's resistance have an impact on the ohmic polarization loss. The resistivity of the building components (collection plates and carbon electrodes) also has an impact. Concentration polarization loss, also known as mass transportation loss, is a phenomena that results from ion propagation across the electrolyte membrane. This lack of transfer of mass of the reactant at the electrode is brought on by the reactant's quick absorption. Particularly when current densities are greater, this loss is significant.

3.2 Proposed NA-WC MPPT

3.2.1 Artificial Neural Network

Artificial neural networks (ANNs), a type of machine learning approach, are designed like the human brain neural networks that are biologically generated seen in the human brain. By replicating the action of linked neurons, ANNs are intended to learn and detect patterns, make predictions, and resolve complicated issues. The fundamental building block of an ANN is the artificial neuron, sometimes referred to as a perceptron. Every neuron gets a single input or multiple inputs, which are subsequently multiplied by the appropriate values. The result of the neuron is then determined by passing these weighed inputs through a function of activation. Additional neurons in a network may also receive its result. Back propagation is a technique used in artificial neural network training. A collection of initial data and their matching goal outcomes are supplied to the neural network throughout training. By contrasting its projected outcomes with the goal outcomes and decreasing the error using optimization techniques like gradient descent, the network continuously modifies the weights and biases of the neurons. The network may learn from its mistakes and get better at making precise forecasts or categorizations thanks to this continuous approach.

3.2.2 Water Cycle Algorithm

Following these 12 steps will enable WCA implementation.

Step 1: M_{gk},M_{pop},d_{max}, and max_$repetition$ are the primary input variables to be initiated.

Step 2: Using the subsequent formulas, the population, streams (raindrops), rivers, and sea are randomly initiated:

$$Population\ of\ raindrops = \begin{bmatrix} sea_1 \\ river_2 \\ Raindrop_2 \\ \vdots \\ Raindrop_{Mpop} \end{bmatrix} = \begin{bmatrix} y_1^1 & y_2^1 & \cdots y_{Mvar}^1 \\ y_1^2 & y_2^2 & \cdots y_{Mvar}^2 \\ \vdots & \vdots & \vdots \\ y_1^{Mpop} & y_2^{Mpop} & \cdots y_{Mvar}^{Mpop} \end{bmatrix} \quad (1)$$

Step 3: Determine the monetary value of each raindrop using the cost function (C) given as follows:

$$V_j = Cost_j = l\left(y_1^j, y_2^j, \dots, y_{Mvar}^j\right) j = 1,2,3, \dots, M_{pop} \quad (2)$$

Where M_{pop} and N_{vars} stand for, accordingly, the starting population (amount of raindrops) and the quantity of design factors. The contents of each choice factor (y_1; y_2; y_3;…; y_{Nvar}) are shown as numbers in floating points. The sea and rivers receive the finest raindrop. The total number of raindrops in the sea and rivers is known as the M_{gk}:

$$M_{gk} = NumberofRivers + 1 \quad (3)$$

The equation that follows is used to determine the residual raindrops:

$$M_{Raindrops} = M_{pop} - M_{gk} \quad (4)$$

Step 4: use the following equation to describe the rivers' and the sea's magnitude:

$$MG_m = round\left\{\left|\frac{Cost_m}{\sum_{j=1}^{Mgk} Cost_d}\right| \times M_{Raindrops}\right\}, m = 1,2,..,M_{gk} \quad 5$$

$$V_m = Cost_m - Cost_{Mgk+1}, m = 1,2, \dots, M_{gk} \quad (6)$$

where MG_m is the total number of streams that empty into rivers or the sea.
Step 5: The subsequent equation describes how the rivers and streams interact:

$$Y_{Stream}(d+1) = Y_{Stream}(d) + rand \times V \times \left(Y_{sea}(d) - Y_{Stream}(d)\right) \quad (7)$$

$$Y_{Stream}(d+1) = Y_{Stream}(d) + rand \times V \times \left(Y_{River}(d) - Y_{Stream}(d)\right) \quad (8)$$

Where C is a number close to 2, and $rand$ is a uniformly distributed random variable in the range of 01 to 12. In order to prevent the streams from traveling in different directions, the C value is greater than 1.
Step 6: The Rivers flow in the next formula in the direction of the sea:

$$Y_{River}(d+1) = Y_{River}(d) + rand \times V \times \left(Y_{sea}(d) - Y_{River}(d)\right) \quad (9)$$

Step 7: The ideal approach is to replace the location of a river with a stream.
Step 8: If a river finds a more effective solution than the sea, the positions of the two are switched (in a manner to Step 7).
Step 9: Examine the state of evaporation situation:

$$if\left|Y_{sea} - Y_{River}^j\right| < t_{max} or rand < 0.1 j = 1,2,3, \dots, M_{gk} - 1$$
$$PerformRainingProcess$$
$$endif \quad (10)$$

where t_{max} is a relatively low value to improve the capabilities of the WCA.

The following equation is used to find close to perfect solutions for streams that flow approaching the sea.

$$if\left|Y_{sea} - Y_{Stream}^j\right| < t_{max} j = 1,2,3, \dots, MG_m$$
$$PerformRainingProcess$$
$$endif \quad (11)$$

In order to create a new population moving in an alternate direction, the rainfall method is used.
Step 10: Verify the evaporation criterion; if it is met, rainfall will take place to create a new stream.

$$Y_{Stream}^{new}(d+1) = LB + rand \times (UB - LB) \quad (12)$$

Where, accordingly, the upper bound (UB) and lower bound (LB) serve as the top and bottom boundaries.
Step 11: Apply the equation below to lower the value of the customized variable t_{max}:

$$t_{max}(d+1) = t_{max}(d) - \frac{t_{max}(d)}{Max.iteration} \quad (13)$$

Step 12: Converge criteria should be checked. If it is met, the algorithm will have terminated; otherwise, move back to Step 5.

The WCA was utilized in this work to identify the ANN algorithm's ideal weights. As a result, it suggested the WCA-ANN, a novel hybrid method, to solve the classification issues. The ANN algorithm generates the starting weights at arbitrary to begin the procedure. The ANN model's outcomes are used to multiply the values entered by the appropriate the weights, or w_{ij}.

4. RESULT AND DISCUSSION

The Matlab tool is used to construct and evaluate the representation of the PEM-FC supplied by a booster converter that was created utilizing either fixed or new suggested NA-WC MPPT. (Tables 1 and 2), correspondingly, include the specifications for the 7 kW PEM-FC and the boost converter. The polarizing curve of the 7 kW PEM-FC in use is shown in (Figure 3). The reaction time, overshoot, and ripple effectiveness of the PEM-FC power system are examined using the proposed model.

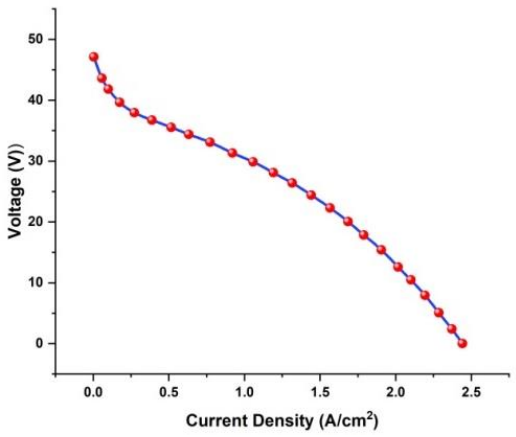

Figure 3. 7 kW PEM-FC Curve Polarization

Table 1. PEM-FC Variables.

Value	Variable
0.4	Oxygen partial pressure O2 (bar)
2.7	Hydrogen partial pressure H2 (bar)
300	Cell active surface (cm^2)
51	No of cells
1.30	Open circuit voltage (V) for a cell
7500	MPP greatest power (W)

Table 2. DC-DC Variables.

Value	Variables
48	Vg (nominal voltage (V))
51	Resistive load (Ω)
11	Switching frequency Fs (kHz)
1500	C (μF)
6	L (mH)

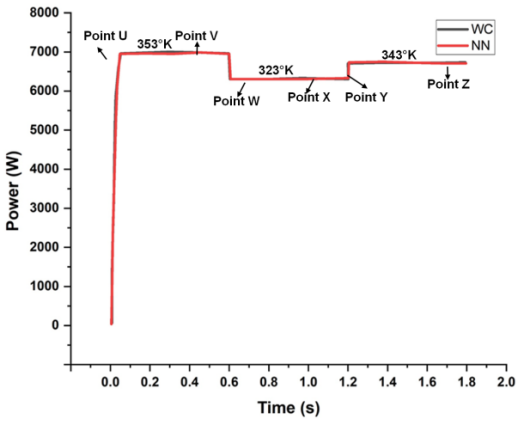

Figure 4. PEM-FC Power Outcomes

The energy output of the PEM-FC is depicted in Figure. 4 utilizing three different types of MPPT: NN and WC. (Figure 4), the PEM-FC temperature is changed to examine the efficiency of WC MPPT regulators. Details concerning the response time, overshoot, and ripple capabilities of the focused in spots (V-Z) are shown in Figure. 5-7.

The suggested NA-WC MPPT has lower overshoot than the traditional WC ones (U, W, and Y), as can be shown in (Figure 5), which makes this distinction quite evident. In all scenarios investigated (U, Wand Y), it is evident from (Figure 6) that the suggested NA-WC MPPT works better than WC MPPT.

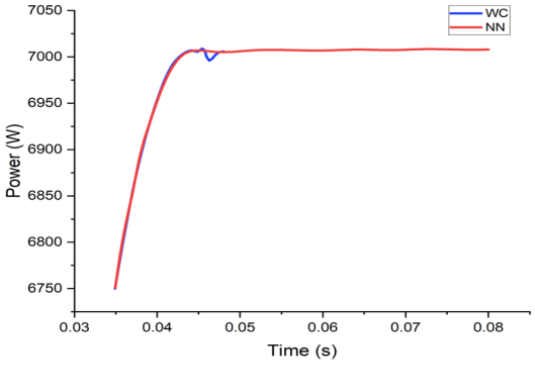

(A) Overshoot at Point U

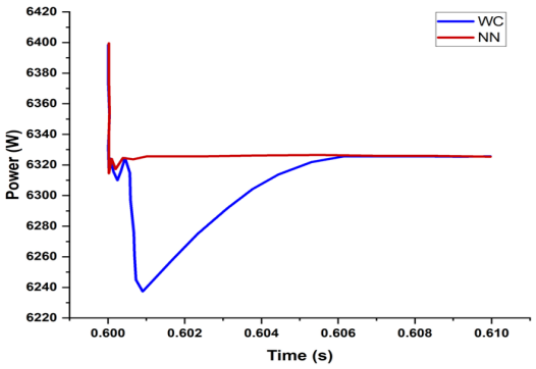

(B) Overshoot at Point W

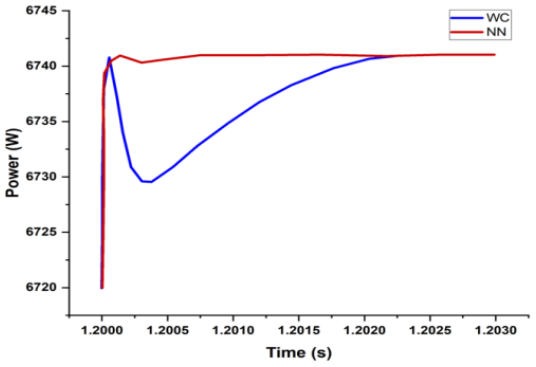

(C) Overshoot at Point Y

Figure 5. PEM-FC Power Outcomes for Overshoot

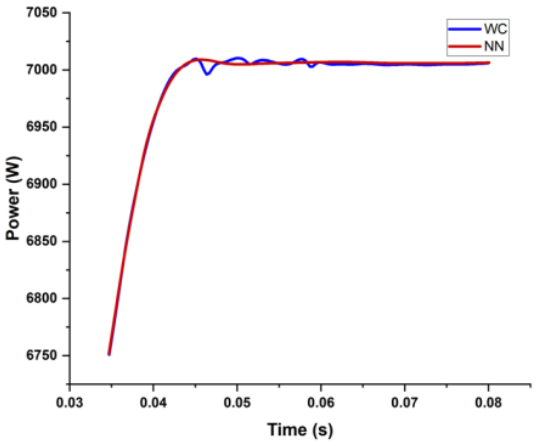

(A) Response Time at Point U

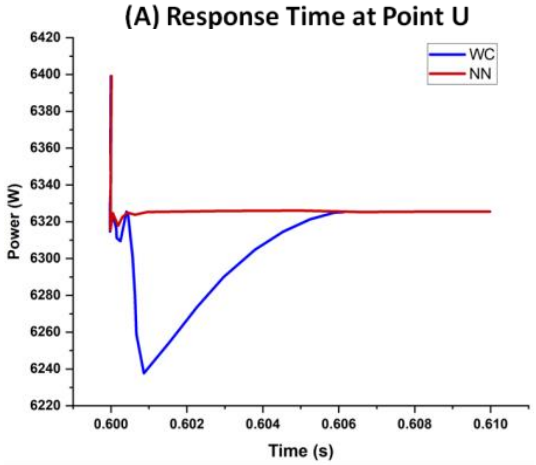

(B) Response Time at Point W

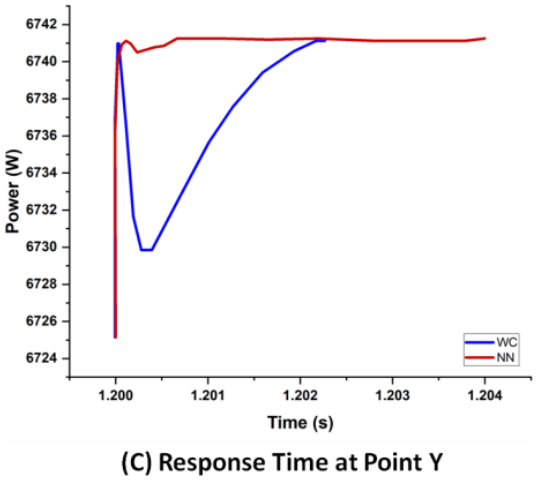

Figure 6. PEM-FC Power Outcomes for Response time

Figure 7 (V, X and Z) shows the ripple for the MPPT controllers. It is unquestionably evident from (Figure. 7) that the suggested NA-WC MPPT controllers minimize the power output ripple in comparison to the traditional WC MPPT regulators.

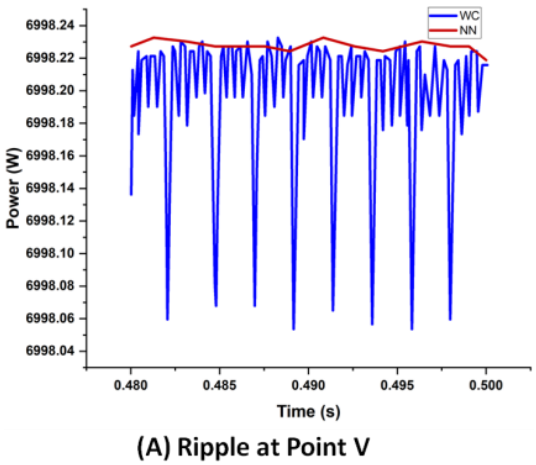

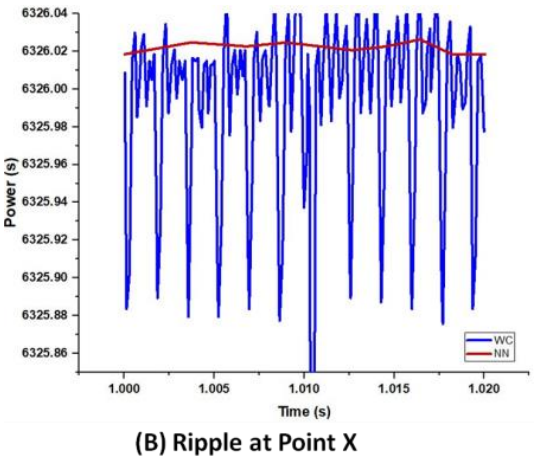

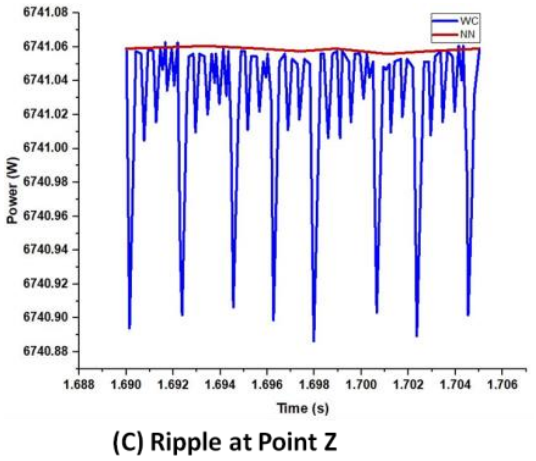

Figure 7. PEM-FC Power Outcomes for Ripple

Table 3 provides a summary of the primary effectiveness enhancements. Table 3 shows that, given the effectiveness metric taken into consideration in both dynamic and stable replies, the suggested NA-WC MPPT outperformed WC MPPTs in all experiment situations.

Table 3. Result summaries.

Overshoot		
Points	Water Cycle (MPPT)	Neural Network
Point U	14 (W)	-
Point W	51(W)	12
Point Y	12(W)	2
Response time		
Point U	50 (ms)	45
Point W	6.2 (ms)	1.3
Point Y	2.2 (ms)	0.8
Ripple (w)		
Point V	0.17(W)	-
Point X	0.16(W)	-
Point Z	0.20(W)	-

5. CONCLUSION

A dynamic-stepped maximum power point tracking (mppt) technology and a neural adaptive water cycle (NA-WC) for the pem-fc power system was suggested in this article. A 7 kW PEM-FC supplied by a boost conversion created utilizing the suggested mppt controller has been effectively used to study the efficacy of the suggested approach. The suggested dynamic-stepped mppt with neural adaptive water cycle improves the overshoots, according to simulation findings obtained through the matlab tool. Additionally, the voltage ripple is significantly reduced by the proposed na-wc mppt regulator. Given that a large ripple current impact causes periodic trips owing to harmonics and even excess electricity, which might shorten the fuel cell's life expectancy, this property is essential to boosting fuel cell effectiveness and preserving its lifespan. The next phase will involve testing the created hardware-in-the-loop neural network mppt controller on an experimental architecture.

References:

Ahmadi, M.H., Ghazvini, M., Alhuyi Nazari, M., Ahmadi, M.A., Pourfayaz, F., Lorenzini, G. and Ming, T., 2019. Renewable energy harvesting with the application of nanotechnology: A review. International Journal of Energy Research, 43(4), pp.1387-1410. https://doi.org/10.1002/er.4282

Aly, M. and Rezk, H., 2020. A differential evolution-based optimized fuzzy logic MPPT method for enhancing the maximum power extraction of proton exchange membrane fuel cells. IEEE Access, 8, pp.172219-172232. https://doi.org/10.1109/ACCESS.2020.3025222

Aly, M. and Rezk, H., 2022. An improved fuzzy logic control-based MPPT method to enhance the performance of PEM fuel cell system. Neural Computing and Applications, pp.1-12. https://doi.org/10.1007/s00521-021-06611-5

Bizon, N., Tabatabaei, N.M., Blaabjerg, F. and Kurt, E., 2017. Energy harvesting and energy efficiency. Technology, Methods, and Applications, 37. https://doi.org/10.1007/978-3-319-49875-1

Chong, Y.W., Ismail, W., Ko, K. and Lee, C.Y., 2019. Energy harvesting for wearable devices: A review. IEEE Sensors Journal, 19(20), pp.9047-9062. https://doi.org/10.1109/JSEN.2019.2925638

Gul, H., Raza, W., Lee, J., Azam, M., Ashraf, M. and Kim, K.H., 2021. Progress in microbial fuel cell technology for wastewater treatment and energy harvesting. Chemosphere, 281, p.130828. https://doi.org/10.1016/j.chemosphere.2021.130828

Haq, I.U., Khan, Q., Ullah, S., Khan, S.A., Akmeliawati, R., Khan, M.A. and Iqbal, J., 2022. Neural network-based adaptive global sliding mode MPPT controller design for stand-alone photovoltaic systems. Plos one, 17(1), p.e0260480. https://doi.org/10.1371/journal.pone.0260480

Hussaian Basha, C.H. and Rani, C., 2020. Performance analysis of MPPT techniques for dynamic irradiation condition of solar PV. International Journal of Fuzzy Systems, 22(8), pp.2577-2598. https://doi.org/10.1007/s40815-020-00974-y

Jadhav, D.A., Mungray, A.K., Arkatkar, A. and Kumar, S.S., 2021. Recent advancement in scaling-up applications of microbial fuel cells: from reality to practicability. Sustainable Energy Technologies and Assessments, 45, p.101226. https://doi.org/10.1016/j.seta.2021.101226

Liang, J., Zhu, G., Wang, C., Wang, Y., Zhu, H., Hu, Y., Lv, H., Chen, R., Ma, L., Chen, T. and Jin, Z., 2017. MoS2- based all- purpose fibrous electrode and self- powering energy fiber for efficient energy harvesting and storage. Advanced Energy Materials, 7(3), p.1601208. https://doi.org/10.1002/aenm.201601208

Luta, D.N. and Raji, A.K., 2019. Fuzzy rule-based and particle swarm optimisation MPPT techniques for a fuel cell stack. Energies, 12(5), p.936. https://doi.org/10.3390/en12050936

Priyadarshi, N., Azam, F., Solanki, S.S., Sharma, A.K., Bhoi, A.K. and Almakhles, D., 2021. A bio-inspired chicken swarm optimization-based fuel cell system for electric vehicle applications. Bio-inspired neurocomputing, pp.297-308. DOI: 10.1007/978-981-15-5495-7_16

Rezk, H., Aly, M. and Fathy, A., 2021. A novel strategy based on recent equilibrium optimizer to enhance the performance of PEM fuel cell system through optimized fuzzy logic MPPT. Energy, 234, p.121267. https://doi.org/10.1016/j.energy.2021.121267

Sarhan, M.A., Ding, M., Chen, X. and Wu, M., 2017, December. Performance Study of Neural Network and ANFIS Based MPPT Methods For Grid Connected PV System. In Proceedings of the 2017 VI International Conference on Network, Communication and Computing (pp. 227-234). https://doi.org/10.1145/3171592.3171623

Tang, C., Zhao, Y., Kang, C., Yang, Y., Morgan, D. and Xu, L., 2019. Towards concurrent pollutants removal and high energy harvesting in a pilot-scale CW-MFC: Insight into the cathode conditions and electrodes connection. Chemical Engineering Journal, 373, pp.150-160. https://doi.org/10.1016/j.cej.2019.05.035

Shubhendra Pratap Singh
Teerthanker Mahaveer University, Moradabad, Uttar Pradesh, India
shub.pratap16@gmail.com
ORCID 0000-0003-3712-7905

Beemkumar N.
Jain (deemed to be) University, Bangalore, India
n.beemkumar@jainuniversity.ac.in
ORCID 0000-0003-3868-0382

Ganesh Kumar Kantak
Vivekananda Global University, Jaipur, India
ganesh.kantak@vgu.ac.in
ORCID 0000-0002-2604-4947